Engineered Science
DOI: https://dx.doi.org/10.30919/es1517

Strain Rate-Dependent Nonlinear Fractional Order Modeling of Elastomer Polymers: A Comprehensive Power-Law Approach

Zhangda Zhao, Wenjun Meng*and Bijuan Yan*

Abstract

To exactly and comprehensively characterise the stress-strain evolution of elastomer polymers, a continuous power-law variable fractional order constitutive model with full correlation of strain rates is proposed in this study. Firstly, the influence weights of each parameter in the order model on the stress-strain mechanical curve are analyzed, and it is found that the variable order is most affected by the strain rate. Further, the order model between the variable order fraction and the strain rate is compared and discussed in different strain rate ranges, and the strain rate-dependent continuous power-law order model is determined. Then, based on the equivalent criterion of strain rate and relaxation time, the power function relationships between the elastic modulus and relaxation time and the derivative of strain rate are established, thus the fractional order constitutive model is integrated and established. Subsequently, the applicability and accuracy of the strain rate fully correlated fractional constitutive model are verified by using the test data in strain rates of $0.0001s^{-1}$~$9000s^{-1}$. Compared with the existing variable fractional constitutive model, the proposed model has higher accuracy (the *RMSE* is reduced by 4.77 times, the prediction error is less than 0.05%) and faster calculation, and realizes the strain rate sensitivity prediction of material mechanical properties.

Keywords: Fractional order constitutive model; Strain rate-dependent behavior; Mechanical properties; Elastomer polymers.
Received: 14 April 2025; Revised: 06 May 2025; Accepted: 15 May 2025.
Article type: Research article.

1. Introduction

Elastomer polymers are integral to high-performance applications in fields such as aerospace (*e.g.*, hydraulic pipeline systems in aircraft),[1,2] transportation engineering,[3] mining machinery,[4] and marine technology, including submarines and ships.[5-6] These polymers are prized for their exceptional vibration isolation, energy dissipation, and viscoelastic properties. Under time-domain loading, the elastomer polymers undergo a transition from the glassy state to the highly elastic rubbery state, during which they exhibit a combination of elastic and viscous deformation behaviors. This dual behavior underpins their ability to dissipate energy and reduce vibrations effectively. To capture these complex deformation mechanisms, numerous constitutive models have been developed to describe the nonlinear hyper-viscoelastic behavior of elastomer polymers. Importantly, the stress-strain mechanical properties of these materials are significantly influenced by strain rates, which induce phenomena such as strain rate sensitivity, strain softening, and strain hardening. These effects become particularly pronounced under high strains, where polymers exhibit complex nonlinear behavior. Consequently, the development of strain rate-dependent constitutive models is crucial for accurately characterizing and understanding the intricate mechanical responses of elastomer polymers.

The mechanical deformation behaviors have attracted great interests of researchers.[7,8] Over recent decades, researchers have conducted extensive experiments on the nonlinear super-viscoelastic behavior of elastomer polymers under various strain rates,[9,10] and compression or tension loading processes,[11] including polyethylene terephthalate (PET),[12] polyurea,[13,14] high-damping rubber,[15,16] and polyurethane.[17,18] For instance, Boyce *et al*.[19] introduced a strain rate-dependent constitutive model, which was founded on the intricate interplay between the internal molecular orientation and relaxation processes in PET, thereby elucidating its strain rate sensitivity behavior within the low strain rate range. Sarva *et al*.,[20] leveraging both theoretical frameworks and experimental data, constructed a super-viscoelastic constitutive model that accurately characterized the nonlinear

School of Mechanical Engineering, Taiyuan University of Science and Technology, No. 66, Waliu Road, Wanbailin District, Taiyuan City, Shanxi Province, 030024, China
**Email:* s2003110@126.com (B. Yan); tyustmwj1206@126.com (W. Meng)

mechanical behavior of polyurea across a wide range of strain rates and temperatures. Furthermore, Miao *et al*.[21] developed an equivalent mechanical configuration, drawing insights from tensile test data across diverse loading strain rates. Their findings revealed that polyurea exhibited not only a significant strain rate dependency but also intricate strain hardening and large deformation evolution processes within its stress-strain curve.

In addition, the elastomer polymers exhibit different mechanical properties under small and large strains in the glass transition region and the elastomeric state. This is due to the freeze-thaw reorganization of the internal molecular chains in elastomer polymers, which determines the mechanical evolution of the polymers. At small strains, the polymer molecular chains complete all relaxation processes. However, at large deformations, relaxation times are shorter, and the recombination rate between molecular chains starts to increase.[22] To explain this mechanical phenomenon, several molecular network models have been proposed to describe the mechanical response of polymers during large deformations. For instance, Bernard and colleagues developed a molecular chain network model to predict the viscoelastic large deformation state of ultra-high molecular weight polyethylene.[23] Although these models capture the nonlinear hyperelastic and viscoelastic properties of polymers at varying strain rates, they overlook the real-time variation of material constitutive parameters with strain rates. Typically, these parameters are treated as constants, failing to account for the evolution of polymer stress-strain mechanical properties over time, a process that alters and determines the final mechanical properties of the polymers. Therefore, to accurately predict the stress-strain mechanical deformation response of elastomer polymers, their constitutive models must incorporate the strain rate dependence of material parameters and the overall mechanical change processes.

Subsequently, the fractional derivative constitutive model has been effectively validated for fitting the nonlinear superelastic deformation behavior of elastomer polymers under quasi-static tension and compression.[24] Additionally, due to its simplicity and fewer parameters requiring experimental fitting, it has gained widespread application. As application conditions become increasingly complex and variable, Coimbra *et al*.[25] introduced a variable fractional derivative constitutive model to describe the linear elastic deformation of materials, where the order of the fractional derivative varied with time. Meng *et al*.[26] developed a variable fractional order constitutive model to characterize the strain softening behavior of polymers, where the variable fractional order described the trends in a material's mechanical properties. Given that the strain rate influences key material parameters such as the elastic modulus and relaxation time, Khajehsaeid *et al*.[27] discovered that the relaxation time of rubber materials decreased with increasing strain rates. Meanwhile, Yu *et al*.[28] established a visco-hyperelastic constitutive model across a wide range of strain rates, revealing a positive correlation between the material's elastic modulus and the logarithm of strain rate. At the same time, they characterized the evolution of both elastic modulus and relaxation time using a power function, elucidating the dependence of relaxation time and elastic modulus on strain rate.

Further, considering the evolution of polymer mechanical properties during tensile or compression tests,[29,30] Su *et al*.[31] employed a variable fractional-order constitutive model to study the nonlinear stress-strain relationships under varying strain rates and loading conditions. This model incorporated both time and strain variables into the variable fractional order, demonstrating its capability to characterize the changes in polymer mechanical properties. Afterwards, the model was extended by Cai *et al*.,[32] who formulated the variable fractional order as a power function dependent on strain. Drawing on experimental loading data across different strain rates, they introduced a fractional-order constitutive model with a continuously variable power-law order to characterize the complete deformation process of elastomer polymers. The model's elastic modulus and relaxation time parameters accounted for the material's sensitivity to strain rates. However, the above variable fractional order did not account for strain rate-dependent effects.

Consequently, this study introduces a strain rate-dependent variable fractional-order constitutive model to elucidate the comprehensive strain rate-dependent nonlinear mechanical response of elastomer polymer materials. This model not only correlates material parameters with strain rates but also allows the order determining material mechanical trends to vary in real-time with the strain rate.

The structure of this paper is organized as follows: Section 2 analyses the parameter characteristics and weight influences of variable fractional order. Section 3 discusses the strain rate-dependent variable fractional order models for low, medium, and high strain rates, proposing a strain rate-independent variable fractional order constitutive model to describe and predict the nonlinear behavior of elastomer polymers. In Section 4, the proposed model's suitability for characterizing mechanical responses at both low and high strain rates is demonstrated, followed by validation of its applicability and predictive accuracy using test data across a wide range of strain rates. Section 5 contains the discussion and conclusions.

2. Characteristics analysis of the order in the variable fractional-order constitutive model

2.1 Variable fractional-order constitutive model

Rubber polymers exhibit both hyperelastic and viscoelastic nonlinear response characteristics. Currently, the elastic pot element is commonly employed to characterize the complex nonlinear stress-time-strain behavior, replacing the spring and viscoelastic pot elements. The constitutive relationship of this element not only reduces the model's parameter count but also enhances its applicability. The constitutive relationship in the form of variable fractional order is:

Fig. 1: Tensile specimens of fluororubber (FKM) and silicon rubber (SR), and Instron 68TM-50 testing machine.

$$\sigma(t) = E\tau^{\alpha(t)} \frac{d^{\alpha(t)}\varepsilon(t)}{dt^{\alpha(t)}}, 0 \le \alpha(t) \le 1 \quad (1)$$

where E is the modulus of elasticity of the material, τ is the relaxation time, t is the loading time, $\varepsilon(t)$ denotes the strain, $\sigma(t)$ denotes the stress, $\alpha(t)$ represents the order of the fractional derivative spring pot element, which is capable of describing the evolution trend of the curve of the complex mechanical properties of the rubber deformation over time, and it is valued in the range of 0~1. When $\alpha(t)$=0, the spring pot element transforms into a linear spring element. When $\alpha(t)$=1, it corresponds to a viscous damping pot.

After conducting quasi-static tests, as shown in Fig. 1, it is discovered that the stress-strain response of elastomer polymers exhibits a power-law curve pattern, while the relaxation modulus also demonstrates a power-law behavior:[21]

$$E(t) = \frac{E}{\Gamma(1-\alpha(t))}\left(\frac{t}{\tau}\right)^{-\alpha(t)} \quad (2)$$

where Γ(•) represents the gamma function.

Therefore, combining the Boltzmann superposition principle and Eq. (2), Eq. (1) can be effectively transformed into the following form:

$$\sigma(t) = E\tau^{\alpha(t)}\Gamma\big(1-\alpha(t)\big)D^{\alpha(t)}\varepsilon(t), 0 \le \alpha(t) \le 1 \quad (3)$$

where $D^{\alpha(t)}$ represents the fractional derivative operator.

To further observe the viscoelastic time-domain response characteristics of elastomer polymers, the strain rate is incorporated into Eq. (2).[33] Subsequently, through mathematical manipulations, an enhanced expression of Eq. (2) can be derived as follows Eq. (4):

$$\sigma(t) = \frac{E\dot{\varepsilon}(t)\tau^{\alpha(t)}}{\Gamma\big(2-\alpha(t)\big)}t^{1-\alpha(t)}, \ 0 \le \alpha(t) \le 1 \quad (4)$$

where $\dot{\varepsilon}(t)$ represents the strain rate.

As is shown in Fig. 2(a), various forms of α are employed to characterize the stress-strain response of polymers. Notably, the order α exhibits a dynamic nature, fluctuating with strain deformation and the progression of time. Specifically, an α value of 0 encapsulates the pure elastic response of the

material, whereas an α value of 1 encapsulates its pure viscous response. However, for nonlinear large deformation responses, both a constant order of α=0.5 and a linear fractional order α fail to provide an accurate description. To address this problem, based on the continuum hypothesis and the principle of freezing-thawing and recombination cycles of internal molecular chains in elastomer polymers, we propose a power-law variable fractional order model (PVFOM). This model divides the characteristic curve of a complete deformation cycle of rubber into consecutive small-time intervals, utilizing a variable order to precisely capture the mechanical deformation behavior of elastomer polymers at various stages, particularly highlighting the nonlinear large deformation mechanical response of the material.[32] Furthermore, the strain rate, representing the amount of strain change per unit time, exhibits an inverse proportionality to the loading time. Within the equivalent time interval, the power-law variable fractional order constitutive model, formulated according to Eq. (3), offers a robust calculation tool for analyzing these complex deformation behaviors, as seen in Eqs. (5) and (6) .

$$\sigma(\varepsilon) = \frac{E\dot{\varepsilon}\tau^{\alpha(\varepsilon)}}{\Gamma(2-\alpha(\varepsilon))}\varepsilon^{1-\alpha(\varepsilon)}, 0 \le \alpha(\varepsilon) \le 1, \varepsilon_1 < \varepsilon \quad (5)$$

$$\alpha(\varepsilon) = k\varepsilon^b + Z \quad (6)$$

where ε_1 is the initial loaded small strain. k is a coefficient, b is an exponent, and Z is a constant.

The parameters within the power-law order model significantly influence the trend of the order and the precision of characterizing the stress-strain response of materials. As depicted in Fig. 2(a), the variable fractional order model exhibiting a power exponent of 1.5 exhibits a closer approximation to the actual mechanical response compared to the model with a parameter value of b=0.5. In addition, the PVFOM related to both strain rate and strain in the figure and the PVFOM related only to strain both describe the continuous multi-stage mechanical evolution state of materials within a complete cycle. Given that strain inherently functions as a derivative of strain rate with respect to time, it becomes evident that there exists a inherent relationship between strain rate and order. As shown in Fig. 2(b), the power function fractional order, which is intrinsically linked to strain rate, is capable of encompassing intricate and comprehensive mechanical responses, encompassing linear elasticity, strain softening, strain hardening, and subsequent nonlinear large deformation behaviors.

2.2 The relationship between power-law order and strain rate

To explore the effect of strain rate on the order of the power-law, fluororubber (FKM) specimens were selected for quasi-static uniaxial tensile tests. These specimens were loaded at a constant strain rate, with varying tensile strain rates applied in each test. The strain function is $\dot{\varepsilon}\tau = \varepsilon$, where τ decreases with the increase of $\dot{\varepsilon}$, indicating that the strain rate is a function of relaxation time, which is inversely proportional to the strain rate.

Therefore, by changing the strain rate, the relaxation time of the material can be controlled. When a constant strain rate is applied, it is assumed that $\dot{\varepsilon}$=d, where d is a constant. Here, for ease of calculation, it is assumed that $d\tau$=m under constant strain rate, where m is a constant, and $m = d\tau = d_{ref}\tau_{ref}$, d_{ref} and τ_{ref} represent the reference strain rate and corresponding reference relaxation time, respectively. To quickly obtain the parameters in Eq. (7) and m, it is necessary to convert Eq. (7) into logarithmic form (see Eq. (8)) within the linear small strain range, to obtain the initial order α_1 and the initial elastic modulus E in the linear elastic stage, and then obtain m. The specific calculation process is shown in Fig. 3.

$$\sigma(\varepsilon) = \frac{E(d\tau)^{\alpha(\varepsilon)}}{\Gamma(2-\alpha(\varepsilon))}\varepsilon^{1-\alpha(\varepsilon)}, 0 \le \alpha(\varepsilon) = k\varepsilon^b + Z \le 1,\ \varepsilon_1 < \varepsilon \quad (7)$$

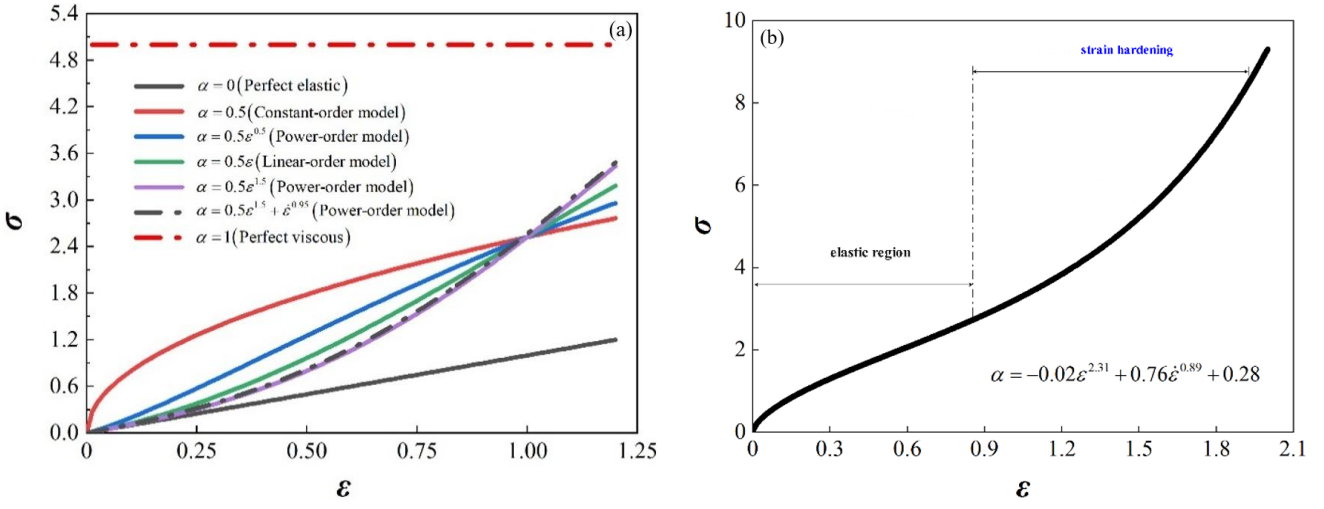

Fig. 2: The influence of the variable-order in different functional forms on stress-strain response. (a) The influence of the variable-order α on the stress-strain response and (b) The strain rate power-law variable-order model describes the multi-stage stress-strain evolution process of polymers.

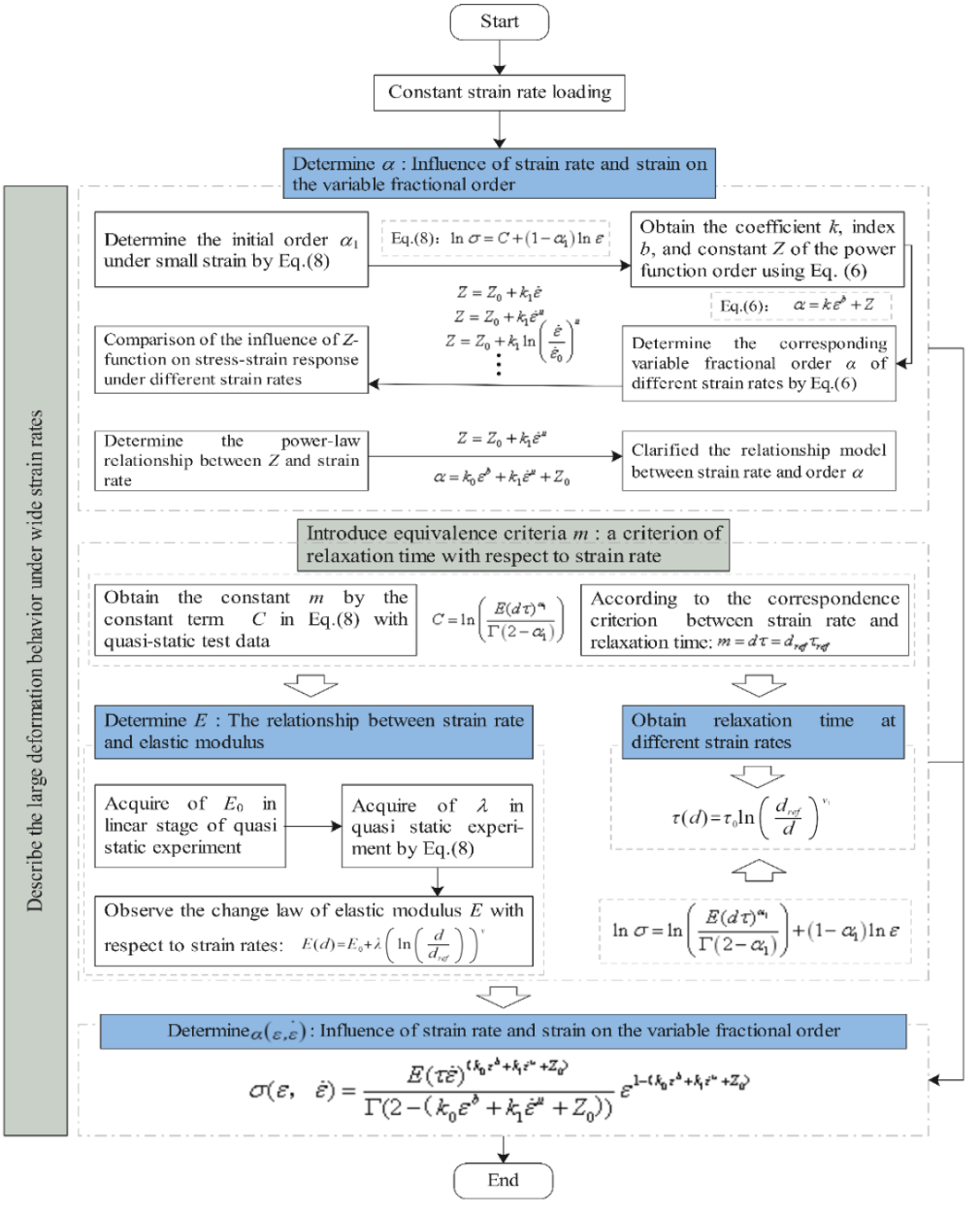

Fig. 3: Flow chart of constitutive model in characterizing strain rate-dependent mechanical behaviors.

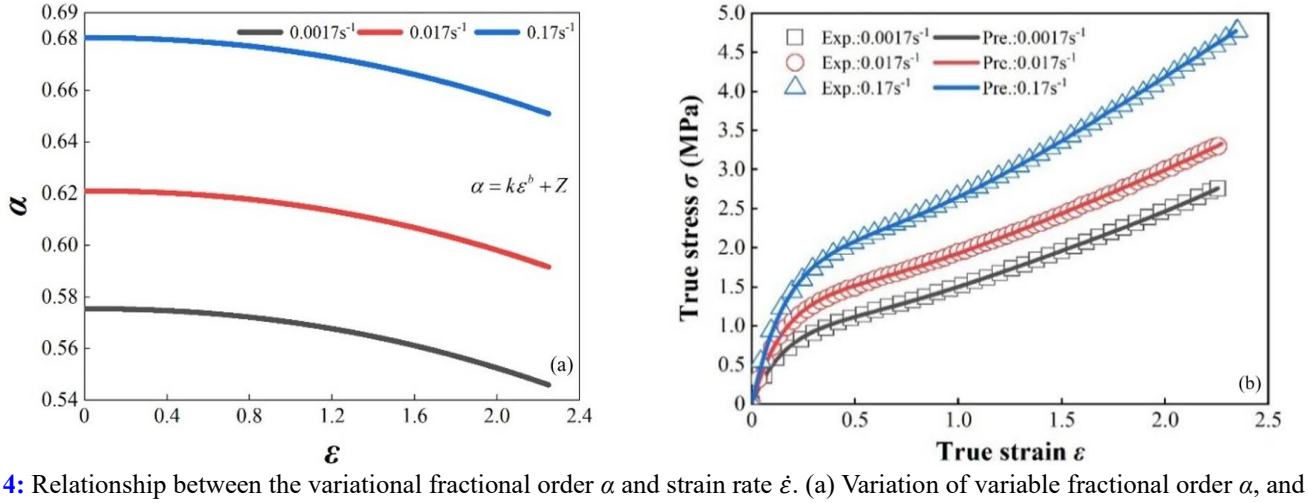

Fig. 4: Relationship between the variational fractional order α and strain rate $\dot{\varepsilon}$. (a) Variation of variable fractional order α, and (b) Stress-strain response of FKM.

$$ln\,\sigma = C + (1-\alpha_1)\,ln\,\varepsilon\,, 0 < \alpha_1 < 1, 0 < \varepsilon < \varepsilon_1,$$
$$C = ln\left(\frac{E(d\tau)^{\alpha_1}}{\Gamma(2-\alpha_1)}\right) > 0 \quad (8)$$

where α_1 can be obtained from the slope (1-α_1); E and τ can be obtained by fitting the stress-strain curve in the linear phase (ε<ε_1) of the quasi-static test.

According to phenomenological theory, it is found that the elastic modulus E exhibits a power-law variation trend with ln(d/d_{ref}). Therefore, the strain rate-dependent expression for the elastic modulus E is obtained using Eq. (9):

$$E = E_0 + \lambda\left(ln\left(\frac{d}{d_{ref}}\right)\right)^{\nu} \quad (9)$$

where the coefficients λ and E_0, as well as the exponent ν, are all constants.

Fig. 4(a) shows the power-law variation curves of the order with strain for FKM at three strain rates of 0.0017s^{-1}, 0.017s^{-1}, and 0.17s^{-1}. It can be seen that the initial order is 0.575 at 0.0017s^{-1}, 0.62 at 0.017s^{-1}, and 0.68 at 0.17s^{-1}. Under the same strain, the order α increases significantly with the increase of strain rate. In summary, there is a functional relationship between the order α and the strain rate. In addition, under the three constant strain rates, α decreases with the increase of strain, and the three fractional orders show a unified power-law decline trend. Fig. 4(b) shows the multi-stage mechanical response of FKM described by the strain rate-dependent power-law order. This model can accurately predict the experimental data of FKM during quasi-static tension. The stress-strain curves predicted by the power-law variable fractional order α corresponding to the three strain rates in Fig. 4 are fully compared with the actual stress-strain responses measured by experiments. It can be found that the power-law variable fractional constitutive equations at the three strain rates accurately and completely predict the stress-strain responses of FKM at each stage, including strain softening, strain hardening, and nonlinear large deformation responses, with an error accuracy of <0.01%.

2.3 Analysis of parameter characteristics order

To comprehensively explore the strain rate dependence of order, it is first necessary to clarify the parameter characteristics of the power-law order, that is, the sensitivity of each parameter to the order. Therefore, this section qualitatively studies the influence of weight and regularity of each parameter on the power-law order α, based on a set of stress-strain data from a quasi-static tensile test (data from the literature).[2] The parameter values were determined through fitting Eq. (7), with an elastic modulus of E=7.56MPa and a relaxation time of τ=0.133s. Three distinct parameter values were designed for the coefficient k, exponent b, and constant term Z of the power-law order α (see Table 1). Based on this, the influence of the three parameters on the stress-strain curve is discussed.

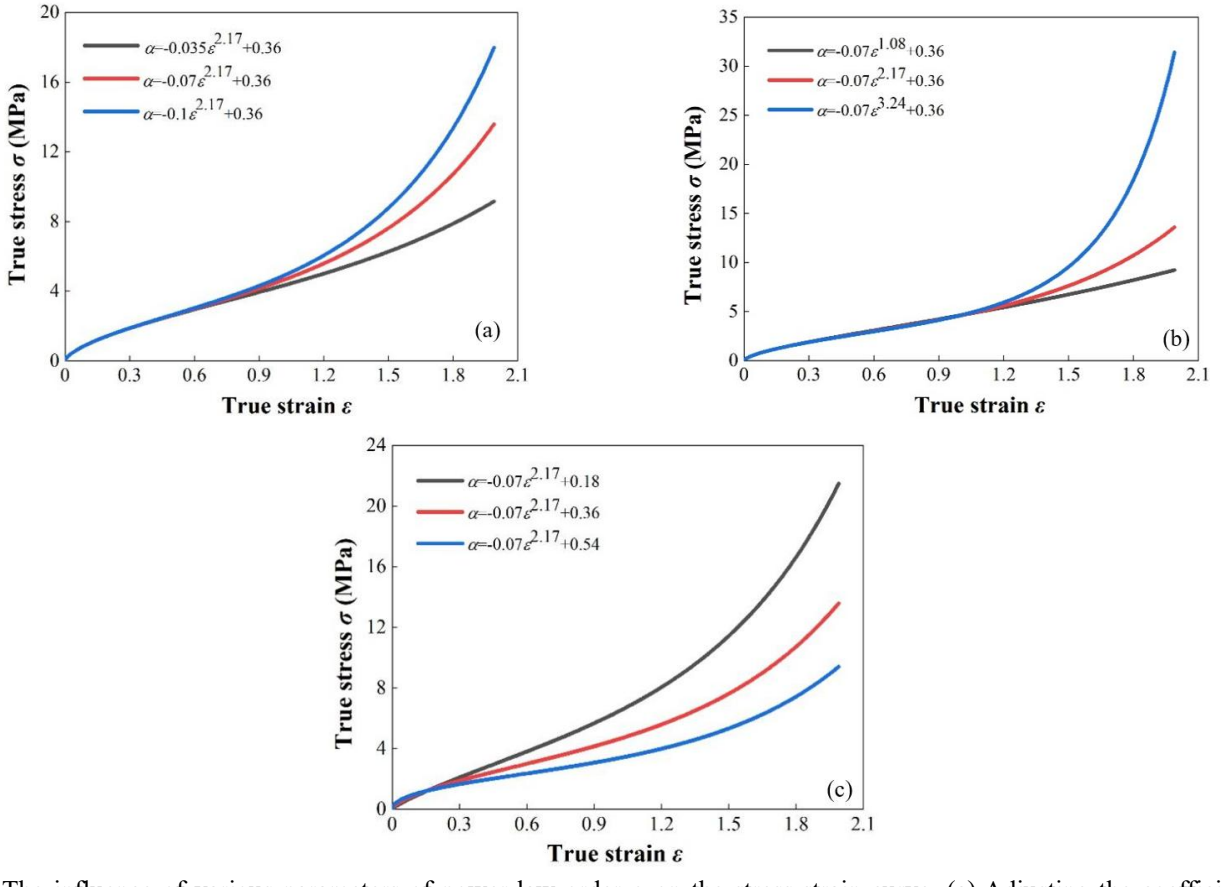

Fig. 5: The influence of various parameters of power-law order α on the stress-strain curve. (a) Adjusting the coefficient k, (b) Adjusting the exponent b, and (c) Adjusting the parameter Z.

Table 1: Three-parameter qualitative analysis scheme for power-law order α.

Type	Scheme 1			Scheme 2			Scheme 3		
k	-0.035	-0.07	-0.1	-0.07			-0.07		
b	2.17			1.08	2.17	3.24	2.17		
Z	0.36			0.36			0.18	0.36	0.54

Fig. 5 qualitatively analyzes the impact of three parameters within the power-law order α on the mechanical response of polyurea composite materials. The results indicate that, under the condition of controlling a single variable while keeping the other two parameters constant, the value of Z exerts the most significant influence on the true stress-strain curve of polyurea. In Fig. 5(a), it becomes evident that, with the exponent b and constant Z remaining unchanged, sole adjustments in the coefficient k lead to a marked upward trend in the order α. Notably, a higher absolute value of coefficient k corresponds to a more pronounced manifestation of the polymer's hyperelastic nonlinear large deformation characteristics. Furthermore, a greater absolute value of coefficient k corresponds to a more pronounced superelastic nonlinear large deformation in the polymer. Notably, the trend of increasing stress-strain response among different coefficients begins to diverge after ε=0.6, marking the transition zone between strain hardening and nonlinear large deformation. Meanwhile, Fig. 5(b) focuses solely on varying the exponent b. As b increases, the stress-strain response of the material gradually intensifies. Particularly when ε exceeds 1.2, the stress-strain curves exhibit distinct changes among different exponents. Notably, the true stress associated with b=3.24 exhibits an exponential surge with strain.

As depicted in Fig. 5(c), a noticeable variation in the mechanical response across the entire strain range is observed with the increase in Z value. Specifically, when the other two parameters are kept constant and only the constant Z is adjusted, it can be found that the response relationship between the true stress and the true strain shows a tendency to weaken gradually as Z increases. This observed variation is intimately linked to the positive and negative values of the parameters present in Eqs. (6) and (7). Concurrently, the adjustment of constant Z results in an enhancement of stress-strain curves across various power-law orders throughout the entire strain range. This contrasts with the strain evolution processes depicted by the coefficient k in Fig. 5(a) and the exponent b in Fig. 5(b), where significant changes in material stress occur only after multiple strain stages.

Furthermore, it can be inferred from the figure that the order α is influenced not only by strain variations but also significantly by strain rates. Additionally, all three parameters in Eq. (6) exhibit a correlation with strain rates, with constant Z demonstrating particular sensitivity to both strain rates and strains. Remarkably, by merely adjusting the power-law order of Z, the constitutive model can approximate the material's evolution throughout the entire deformation process. Therefore, to achieve a more precise characterization of the true stress-strain response of elastomer polymers across a broad range of strain rates, further enhancements to Eq. (6) are necessary. Meanwhile, there is a need to delve deeper into the intricate relationship between the Z value and strain rates, and to establish an order α model that varies concurrently with both strain rates and strains. Such advancements will significantly enhance our ability to accurately understand and predict the mechanical behavior of elastomer polymers under varying strain rates.

3. Construction of strain rate-dependent fractional-order constitutive model for characterizing the nonlinear behavior of elastomeric polymers

To identify a strain rate-dependent fractional-order model (STDFOM) capable of precisely characterizing the nonlinear large deformation response of polymers, this section utilizes the drop weight impact test data of polyurea materials reported in literature at strain rates ranging from 0.001s^{-1} to 1s^{-1} for

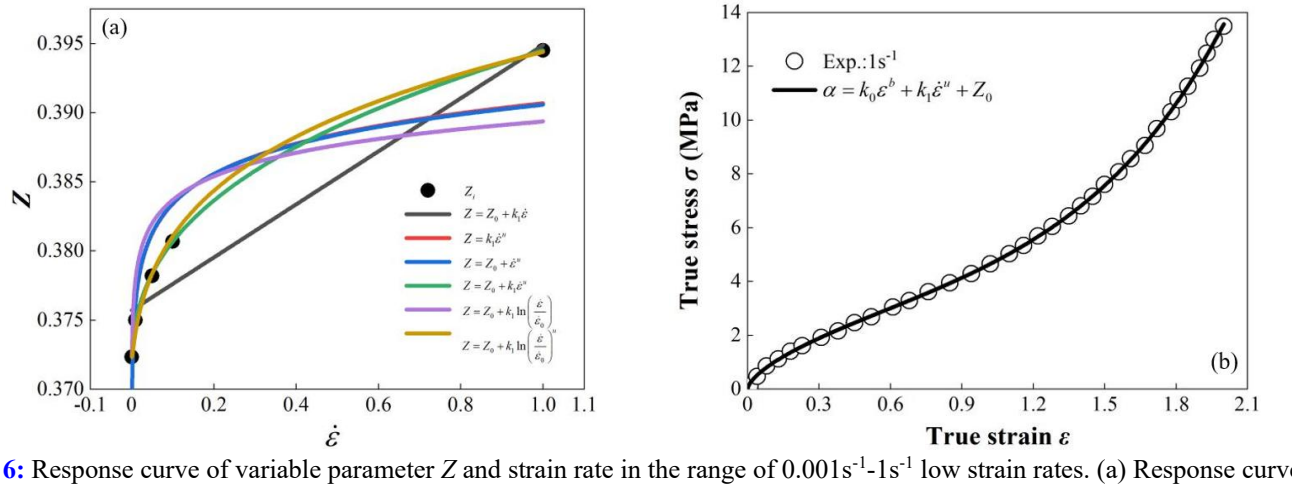

Fig. 6: Response curve of variable parameter Z and strain rate in the range of 0.001s^{-1}-1s^{-1} low strain rates. (a) Response curve of variable parameter Z and strain rate and (b) The predicted true stress-strain curve generated by Z-4 model at a strain rate of 1s^{-1}.

validation.[34] Initially, we explore and analyze various function types of strain rate-dependent continuous power-law fractional-order models within the low strain rate range. Subsequently, the most suitable model is determined by assessing the RSME value of the material's stress-strain curve across each model. Finally, the validated model is generalized and applied to different elastomer polymers for further verification.[35]

3.1 Relationship model between strain rate and fractional order of variation

As shown in Fig. 5(c), the constant term Z in Eq. (6) exhibits a trend characteristic of a power function. Drawing on the equivalent transformation theory, several functional relationships between Z and strain rate are derived in detail in this section, as depicted in Fig. 6(a). A careful examination of Fig. 6(a) reveals that as the strain rate increases, the Z value follows a distinct power-law upward trend. And Table 2 gives characteristics of the relationship between variable Z and strain rate. It is evident that a continuous power-law change function, which is closely tied to the strain rate, offers the most accurate representation of the Z value's actual variation. In comparing various Z-function models, it is noteworthy that the Z-4 and Z-6 power function models stand out as the most effective in terms of prediction. Their predicted trends align closely with the connecting line of the discrete points representing the constant term, effectively capturing the overall trend of the Z value's constant value changes. Conversely, the linear model (Z-1) exhibits the largest prediction gap. Meanwhile, slightly less favorable performance is observed for both power-law models (Z-2 and Z-3) and logarithmic model (Z-5). These models are primarily suitable for describing the Z value at strain rates close to zero; however, as the strain rate increases, the discrepancy in their fitting accuracy becomes increasingly apparent.

Table 2: Characteristics of the relationship between variable Z and strain rate.

Number	Expression	Model constants	R^2
Z-1	$=Z = Z_0 + k_1\dot{\varepsilon}$	2	0.382
Z-2	$=Z = k_1\dot{\varepsilon}^u$	2	0.62653
Z-3	$=Z = Z_0 + \dot{\varepsilon}^u$	2	0.62639
Z-4	$=Z = Z_0 + k_1\dot{\varepsilon}^u$	3	0.99953
Z-5	$=Z = Z_0 + k_1\, ln\left(\frac{\dot{\varepsilon}}{\dot{\varepsilon}_0}\right)$	3	0.60259
Z-6	$=Z = Z_0 + k_1\, ln\left(\frac{\dot{\varepsilon}}{\dot{\varepsilon}_0}\right)^u$	4	0.99582

It is worth noting that the logarithmic models of Z-5 and Z-6 are constructed using the concept of the relationship between the elastic modulus and equivalent ratio of strain rate for reference (as shown in Eq. (9)). However, the introduction of the Z-6 model, which incorporates a continuous power order, resulted in a significant improvement of 39% in the prediction correlation coefficient compared to the Z-5 model, which further confirms that there is a power function relationship between Z and strain rate. As evident from Table 2, among all the models, the Z-4 model stands out with the highest prediction correlation coefficient and a prediction error of less than 0.1%, enabling precise predictions and fittings of Z value variations. Furthermore, compared to the Z-6 model, which boasts a prediction correlation coefficient of 0.99582, the Z-4 model boasts a reduced number of parameters, thereby facilitating a smoother and more efficient fitting calculation process. Consequently, it can be determined that the relationship between the constant term Z and the strain rate in Eq. (6) is accurately captured by the functional relationship outlined in the Z-4 model in Eq. (10). This relationship accurately captures the variation of Z value with strain rate, thereby offering robust support for subsequent analysis and applications.

$$Z = k_1\dot{\varepsilon}^u + Z_0 \tag{10}$$

where the coefficient k_1, the exponent u, and the constant Z_0 are constants, which are experimentally measured data, obtained from the conversion of the compression rate or the impact velocity, and in order to facilitate the calculations, therefore set $\dot{\varepsilon} = d$, with d being a constant (in agreement with the previous section).

3.1.1 Order model of rate-dependent power-law variation in the low strain rate range

Fig. 6(b) shows the prediction of the real stress-strain evolution process of polyurea elastomer (PE) utilizing a continuous power-law variable-order model that incorporates the strain rate and strain co-correlation characteristics of the Z-4 model. It can be seen that the prediction curves generated by the optimised continuous variable order model fit perfectly with the test data curves at a strain rate of $1s^{-1}$, thereby affirming the accuracy of the STDFOM in capturing the intricate real-time variations of PE throughout its entire mechanical deformation phase. This includes the subtle strain behavior observed during the initial compression stage, as well as the subsequent nonlinear large strain response. Furthermore, a comparative analysis of the relationship between variable Z and strain rate presented in Fig. 6(a) further elucidates the suitability of the strain rate power-law variable-order model in describing the stress-strain relationship. Consequently, combining Eq. (10), an enhanced continuous power-law variable-order model that comprehensively accounts for both strain rate and strain correlation is derived as follows:

$$\alpha(\varepsilon, \dot{\varepsilon}) = k_0\varepsilon^b + k_1\dot{\varepsilon}^u + Z_0 \tag{10}$$

where the coefficient k_0 is a constant.

To validate the applicability of the Z-4 model for elastomer polymers, this study conducted an in-depth analysis of the

quasi-static tensile data of two rubber types, silicone rubber (SR) and fluororubber (FKM), within a strain rate range of $0.0017s^{-1}$ to $0.17s^{-1}$. Notably, the elastic modulus of FKM is 1.5 times greater than that of SR, while its hardness is 1.2 times higher. Fig. 7(a) provides a clear representation of the relationship between Z and $\dot{\varepsilon}$ of SR. It is evident from the figure that as the strain rate increases, the variable Z exhibits a power-law upward trend, which aligns with the trend observed in PE materials. Furthermore, a comparative analysis of the predictive capabilities of the Z-4 and Z-6 variable models was conducted. The findings reveal that the Z-4 variable model demonstrates remarkable accuracy, with nearly zero prediction error, enabling precise predictions of individual Z values and anticipation of Z's changing trends. Conversely, the Z-6 variable model is capable of encompassing the original Z values only within a narrow strain rate range of 0 to $0.02s^{-1}$. Beyond this threshold, the prediction error of the Z-6 model gradually increases.

The relationship between Z and $\dot{\varepsilon}$ in FKM depicted in Fig. 8(a) coincides closely with the observations presented in Fig. 7(a), which further verifies the superior predictive accuracy of the Z-4 variable model compared to the Z-6 variable model. Fig. 7(b) provides a detailed examination of the stress-strain mechanical response predictions generated by the strain rate-dependent fractional-order constitutive model incorporating the Z-4 variable model (Eq. (11)) across three distinct strain rates: $0.0017s^{-1}$, $0.017s^{-1}$, and $0.17s^{-1}$. The results show that the prediction curves of this constitutive model are in perfect agreement with the test data, and the average RSME under the three strain rates is less than 0.5%, which shows an excellent prediction performance. Furthermore, Fig. 8(b) extends the analysis to show the predictive effectiveness of the strain rate-dependent fractional-order constitutive model (STDFOCM) on the stress-strain mechanical response of FKM across the same three strain rates. Compared with the original test data, it is found that the prediction curve of the constitutive model is also in good agreement with the test data, and the average RSME at three strain rates is less than 1%, which further

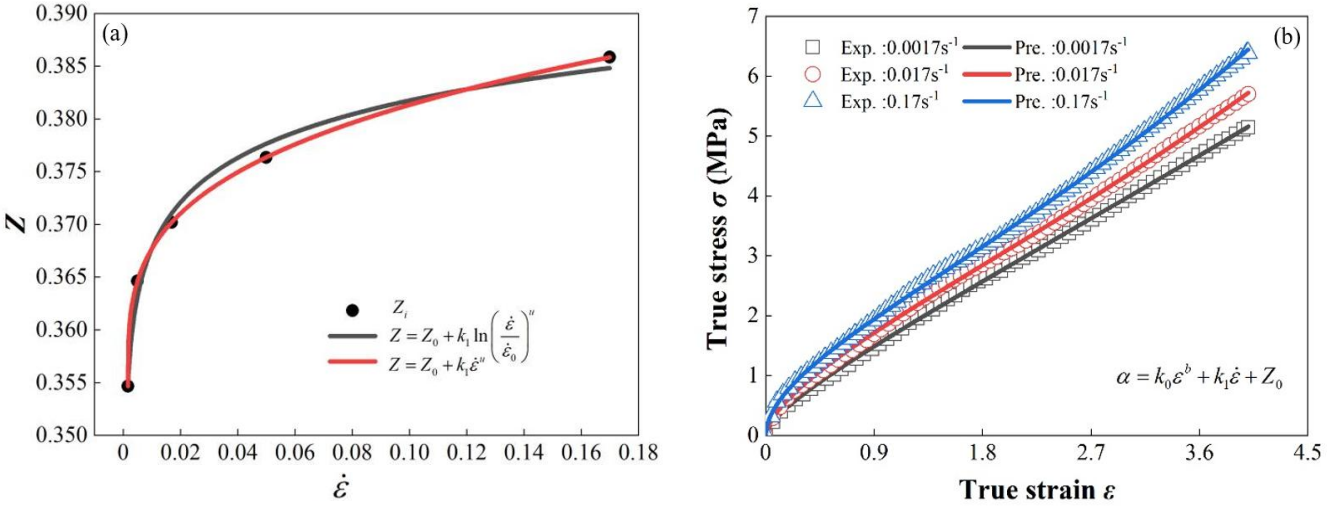

Fig. 7: Prediction efficacy of the strain rate-dependent fractional-order model on SR mechanical response. (a) the correlation between variable Z and strain rate and (b) the correlation between variable Z and strain rate.

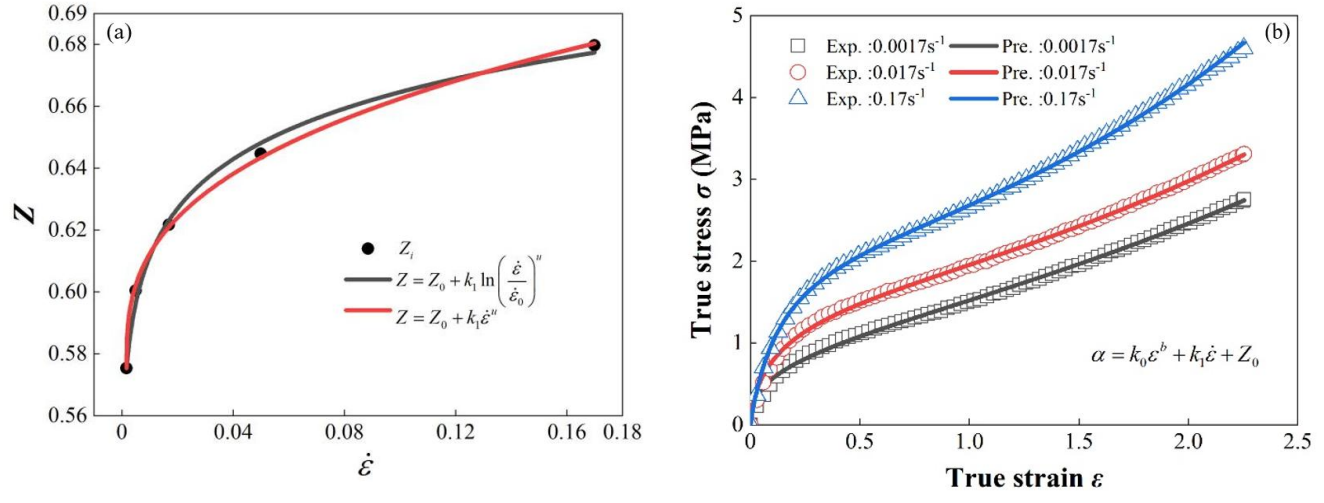

Fig. 8: Prediction efficacy of the strain rate-dependent fractional-order model on FKM mechanical response. (a) The correlation between variable Z and strain rate and (b) Z-4 variable-order model.

verifies the effectiveness and accuracy of the constitutive model.

To delve deeper into the variation of order with strain rate and strain, the tensile test data of SR and FKM at low strain rates were further analyzed, drawing upon the research findings presented in Figs. 7 and 8. As shown in Fig. 9(a), under the strain rates of 0.0017s^{-1}, 0.017s^{-1}, and 0.17s^{-1}, the order α exhibits a power-law decline trend with increasing strain. Simultaneously, the order α increases with a rise in strain rate, accompanied by alterations in its parameters. This observation contradicts prior research that postulated fixed parameters within α. Notably, the order α ranges from 0 to 1, with α=0 indicating linear spring-like material behavior and α=1 signifying linear damper-like characteristics. Consequently, the hyper-viscoelastic properties of materials can be modulated through the manipulation of strain rates.

Fig. 9(b) shows the evolution of the variable fractional order of FKM with strain across three distinct strain rates: 0.0017s^{-1}, 0.017s^{-1}, and 0.17s^{-1}. It can be observed that the variable fractional order α of FKM varies with the increase in strain and strain rate, exhibiting a consistent trend with SR. However, unlike SR, FKM demonstrates a downward convex power-law trend, whereas SR exhibits a downward concave power-law trend. In addition, at the same strain rate, the ratio of α at the initial strain of FKM and SR is greater than 1.5. These phenomena are influenced by the mechanical constitutive properties of the materials: the change of strain rate will change the overall shape of materials, and further affect the mechanical parameters of materials and the internal molecular chain state (such as elastic modulus, damping coefficient, relaxation time, etc.). Consequently, it is necessary to further explore the influence of strain rate on order in the range of medium and high strain rate after clarifying the continuous relationship between strain rate and order and its influence on the mechanical response of materials under the condition of low strain rate.

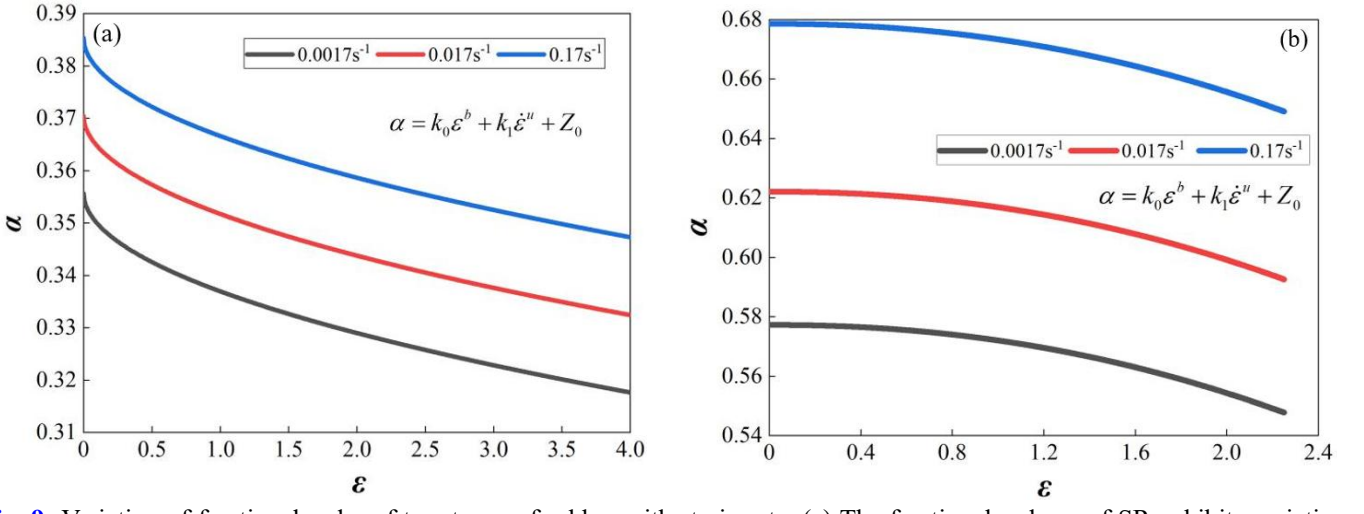

Fig. 9: Variation of fractional order of two types of rubber with strain rate. (a) The fractional order α of SR exhibits variations in response to changes in strain rate and (b) The fractional order α of FKM exhibits variations in response to changes in strain rate.

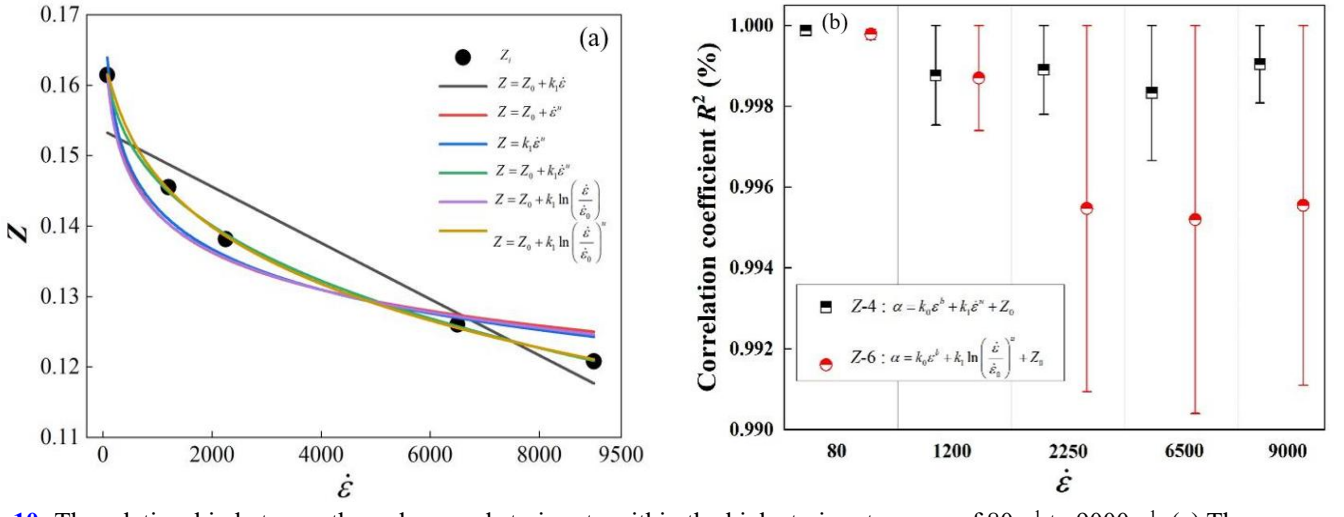

Fig. 10: The relationship between the order α and strain rate within the high strain rate range of 80s^{-1} to 9000s^{-1}. (a) The response curve of Z varying with strain rate and (b) the fitting correlation coefficient for two strain rate-dependent power-law constitutive models.

3.1.2 Order model of rate-dependent power-law variation in the range of medium and high strain rates

In order to prove the variable relationship between strain rate and fractional order α across medium and high strain rate ranges, the SHPB impact compression test data for PET within the range of 80s^{-1} to 9000s^{-1} is used.[13] Fig. 10(a) compares the curves representing different functional forms between variable Z and strain rate with the original Z values across a broad strain rate range. Overall, it is evident that Z exhibits a power-law decrease with increasing strain rate. As the strain rate increases, the Z value decreases, contrary to the trend observed in the low strain rate range. By comparing the predictive characteristics of the functional relationships in Table 2, it becomes apparent that the Z-4 and Z-6 power function models offer the best prediction performance, with prediction accuracies exceeding 99.5%. This finding aligns with the analysis results obtained under low strain rate conditions.

In addition, both models exhibit change curves capable of intersecting the Z value across various strain rates. Nevertheless, with the increase of strain rate, the prediction error of the both models also gradually increases. Notably, the prediction error of the Z-6 model remains lower than that of the Z-4 model, maintaining a prediction accuracy exceeding 99.6% throughout the entire high strain rate range. As shown in Fig. 10(b), within the initial strain rate range of 80s^{-1} to 1000s^{-1}, the prediction accuracy of both models is comparable, approaching 100%. Upon reaching a strain rate of 1200s^{-1}, while the prediction errors of both models remain consistent, the error value increases by approximately 0.1% compared to that at 80s^{-1}. At strain rates of 2250s^{-1} or higher, the prediction error of the Z-4 model surpasses that of the Z-6 model, with an average difference of approximately 0.3%. Given the minimal nature of this error discrepancy, the prediction accuracy of both models can be deemed comparable in engineering calculations. Furthermore, according to Table 2, the Z-6 model possesses one additional constant term parameter compared to the Z-4 model, thereby increasing computational workload. Consequently, it is concluded that the Z-4 model is most suitable for describing the relationship between strain rate and order across a broad range of strain rates, as exemplified in Eq. (11).

3.2 Strain rate-dependent continuous power-law fractional order constitutive model

To accurately depict the mechanical response associated with the strain rate of elastomer polymers, combined with Eq. (11), the fractional variable order model can be extended as:

$$\sigma(\varepsilon,\dot{\varepsilon}) = \frac{E(\dot{\varepsilon})(\tau(\dot{\varepsilon})\dot{\varepsilon})^{\alpha\ (\varepsilon,\dot{\varepsilon})}}{\Gamma(2-\alpha(\varepsilon,\dot{\varepsilon}))}\varepsilon^{1-\alpha(\varepsilon,\dot{\varepsilon})}, \varepsilon > 0, \dot{\varepsilon} > 0 \quad (12)$$

where elastic modulus $E(\dot{\varepsilon})$ and relaxation time $\tau(\dot{\varepsilon})$ are both functions of strain rate, where the elastic modulus is related to strain rate with reference to Eq. (9), and the variable order $\alpha(\varepsilon,\dot{\varepsilon})$ is defined as a power function of strain and strain rate, which is shown in Eq. (11).

For the sake of facilitating calculations, by combining Eqs. (7) and (10), Eq. (12) can be transformed into:

$$\sigma(\varepsilon,d) = \frac{(E_0+\lambda\left(ln\left(\frac{d}{d_{ref}}\right)\right)^{v})(d\tau(d))^{(k_0\varepsilon^b+k_1d^u+Z_0)}}{\Gamma(2-\ (k_0\varepsilon^b+k_1d^u+Z_0)\ )}\varepsilon^{1-\ (k_0\varepsilon^b+k_1d^u+Z_0)}, \varepsilon > 0, d > 0 \quad (13)$$

where $E(d) = E_0 + \lambda\left(ln\left(\frac{d}{d_{ref}}\right)\right)^{v}$, the relaxation time $\tau(d)$, refers to the equivalent conversion, $d\tau = d_{ref}\tau_{ref}$ and its expression is set as $\tau(d) = \tau_0\, ln\left(\frac{d_{ref}}{d}\right)^{v_1}$, where both v and v_1 are constants. Further Eq. (13) can be converted into:

$$\sigma(\varepsilon,d) = \frac{E(d)(\tau(d)d)^{\alpha(\varepsilon,d)}}{\Gamma(2-\alpha(\varepsilon,d))}\varepsilon^{1-\alpha(\varepsilon,d)}, \varepsilon > 0, d > 0 \quad (14)$$

Eq. (14) is referred to as the strain rate-dependent continuous power-law variable fractional-order constitutive model.

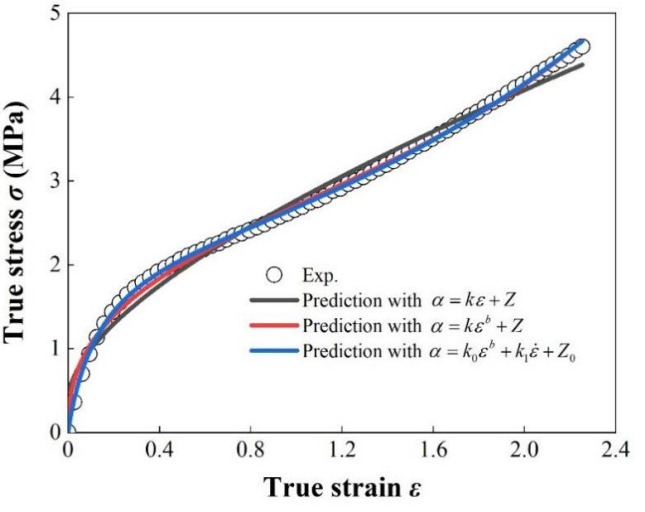

Fig. 11: Stress-strain response of the material characterised by a linear variable fractional order model, a strain dependent power-law variable order model, and a strain and strain rate dependent power-law variable order model (experimental data are obtained at 0.17s^{-1} for FKM).

To further verify the advantages of the constitutive model (Eq. (14)) in predicting the strain-rate-dependent stress-strain mechanical response of materials, three models including the constant term order model, the linear fractional order model, and the strain rate-dependent power function variable order model (STDFOCM) are compared in predicting the stress-strain evolution process of FKM at 0.17s^{-1}. As depicted in Fig. 11, it is evident that the power function order model, which incorporates both strain rate and strain, outperforms both the linear variable order model and the strain-related power-law variable order model. Notably, the stress-strain curve generated by STDFOCM aligns closely with the experimental data, accurately predicting the mechanical response of FKM across various strain intervals.

4. A strain rate-dependent variable fractional order constitutive model across a broad range of strain rates

4.1 A strain rate-dependent variable fractional order constitutive model in the low strain rate range

The hyper-viscoelastic properties of elastomer polymers endow them with unique energy absorption or dissipation capabilities under impact conditions. These materials effectively convert the mechanical energy of external loads into internal work, facilitating energy dissipation. Different impact conditions correspond to a variety of strain rates, and materials exhibit nonlinear large-strain deformation characteristics under these different strain rates. In particular, for elastomer polymers, their mechanical behavior varies significantly with the strain rate. Within the low strain rate range (*e.g.*, 10^{-5} s^{-1}~10^{-1} s^{-1}), the loading time is much longer than the relaxation time of the molecular chains. Under such conditions, rubber molecular chains have sufficient time to rearrange, and the material demonstrates typical viscoelastic properties, with energy absorption primarily relying on the viscous dissipation of the molecular chains.

In contrast, at high strain rates (*e.g.*, $10^{2}s^{-1}$~10^{5} s^{-1}), the loading time is significantly shorter than the relaxation time of the molecular chains. The molecular chains have insufficient time to rearrange, resulting in mechanical behavior dominated by elasticity. At this stage, inertial effects become pronounced, the material's resistance to deformation (stiffness) increases, and due to insufficient dissipation processes, part of the energy is absorbed through elastic recovery or wave propagation.

Based on this distinction, it is essential to conduct in-depth investigations into the mechanical responses of elastomer polymers within both low and high strain rate ranges to uncover their performance characteristics and energy absorption mechanisms under different conditions, providing scientific support for practical engineering applications.

To further investigate the mechanical behavior of materials, we combined predictive modeling with experimental data to determine the variable order of the material, enabling a more accurate description of its mechanical properties. In this study, we proposed a strain-rate-dependent variable fractional-order constitutive model and validated its applicability using compression test data for PET materials in the strain rate range of 0.005 s^{-1}~1 s^{-1}.[19] Experimental results demonstrated that this model effectively captures the fully correlated stress-strain mechanical response at low strain rates.

Additionally, we compared the predictive performance of this model with that of a rate-dependent continuous power-law variable-order model that does not incorporate strain rate effects.[32] The root mean square error (RMSE) was calculated to quantify the fitting deviation between the models and the experimental data. Furthermore, since the adjusted R^2 (R_a^2) comprehensively reflects the overall fitting quality of the model, particularly for complex polymer models, it was jointly used to evaluate the fitting performance of the two models systematically. Detailed results are presented in Tables 3 and 4. This comparative analysis not only highlights the superiority of the proposed model but also provides a novel perspective and tool for investigating the mechanical behavior of elastomer polymers.

Fig. 12(a) provides a detailed exhibition of the prediction curve generated by the strain-dependent continuous power law variable order model for the stress-strain response of PET material across various strain rates. This curve aligns closely with the original experimental data, effectively mirroring the actual deformation trends observed in the material. Nevertheless, when compared to the constitutive model introduced in this paper, there are certain limitations in its predictive capabilities (as evident in Fig. 12(b) and Table 3), particularly during the initial stages of small strain, as well as during strain softening and hardening phases. In contrast, the mechanical response curves predicted by the proposed model are in perfect agreement with the original experimental data, and can fully describe the stress-strain response process of PET materials. Furthermore, across different strain rates, the RSME values associated with the proposed model remain

Table 3: RMSE of two models during 0.005s^{-1}~1s^{-1}.

Models	RMSE at different strain rates				
	0.005s^{-1}	0.01s^{-1}	0.05s^{-1}	0.1s^{-1}	1s^{-1}
$\alpha = k\varepsilon^b + Z$	0.09848	0.03232	0.07899	0.03747	0.18912
$\alpha = k_0\varepsilon^b + k_1\dot{\varepsilon}^u + Z_0$	0.02065	0.02253	0.01839	0.02684	0.04349

Table 4: Adjusted R_a^2 of the two models during 0.005s^{-1}~1s^{-1}.

Models	R_a^2 at different strain rates ($0 \le R_a^2 \le 1$)				
	0.005s^{-1}	0.01s^{-1}	0.05s^{-1}	0.1s^{-1}	1s^{-1}
$\alpha = k\varepsilon^b + Z$	0.99456	0.99697	0.99983	0.99979	0.99779
$\alpha = k_0\varepsilon^b + k_1\dot{\varepsilon}^u + Z_0$	0.99962	0.99984	0.99992	099989	0.99988

consistently lower than those reported by Cai *et al*.[32] This advantage can be attributed to the continuous correlation between the variable order in the proposed model and the strain rate, which further confirms the close relationship between the global stress-strain response of the material and the strain rate.

The results of Fig. 12 and Tables 3 and 4 further demonstrate the applicability of the proposed model in characterizing fully strain-rate-dependent stress-strain mechanical responses within the low strain rate range. Notably, under strain rates of $0.005s^{-1}$ ~ $0.05s^{-1}$, the RMSE ratio between the two models is particularly significant, reaching 4.77 and 4.31 times, respectively. A comparison of the adjusted R_a^2 values at different strain rates reveals that the R_a^2 values of the proposed model consistently exceed 0.9996, corresponding to a prediction error of only 0.04% relative to the experimental data. This indicates that even when accounting for parameter complexity, the proposed model maintains a high fitting accuracy, with predictions nearly matching the true material behavior.

4.2 A strain rate-dependent variable fractional order constitutive model in the high strain rate range

The aforementioned content shows the precise predictive capability of the proposed strain rate-dependent constitutive model in simulating the mechanical response of elastomer polymers within the low strain rate range. In this section, the prediction ability of the constitutive model for the stress-strain curve under the influence of high strain rate is mainly explored. Given the exceptional performance of elastomer polymers in vibration reduction and energy absorption, they are frequently utilized as protective layers against impact and vibration. Furthermore, their mechanical properties associated with high strain rates have garnered extensive research interest. To validate the applicability of the constitutive model proposed in this paper under high strain rates and assess the accuracy of its mechanical response characterization, combined with the data from the impact compression stress-strain tests of PET conducted at strain rates ranging from $80s^{-1}$ to $9000s^{-1}$, as reported in the literature.[13] Both the strain-dependent fractional order constitutive model employed by Cai *et al*.[32]

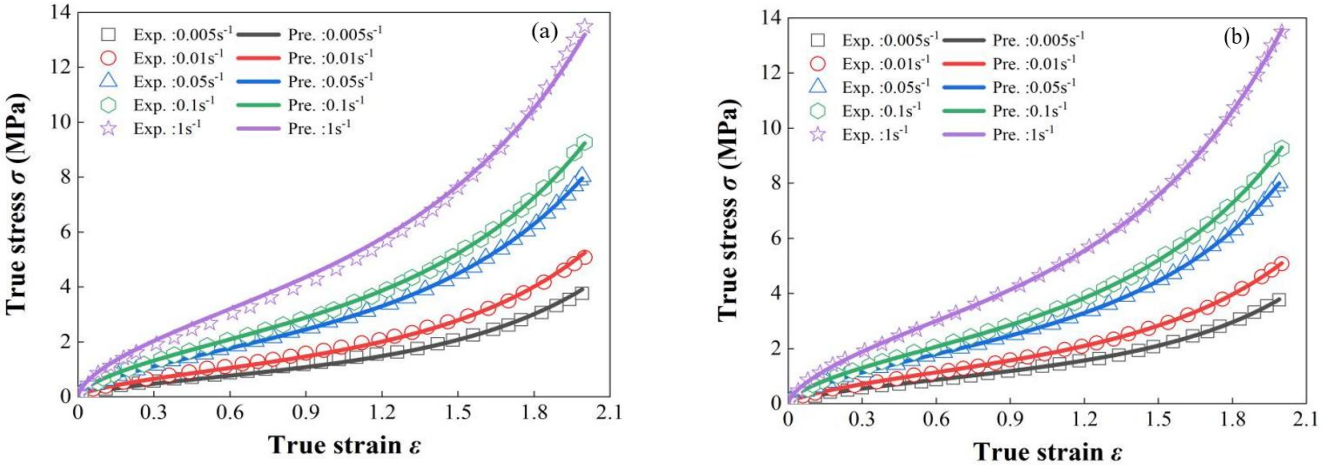

Fig. 12: Stress-strain response comparision in the low strain range of PET using a model (Cai and Wang[32]) (a) and the proposed STDFOCM model in this study (b).

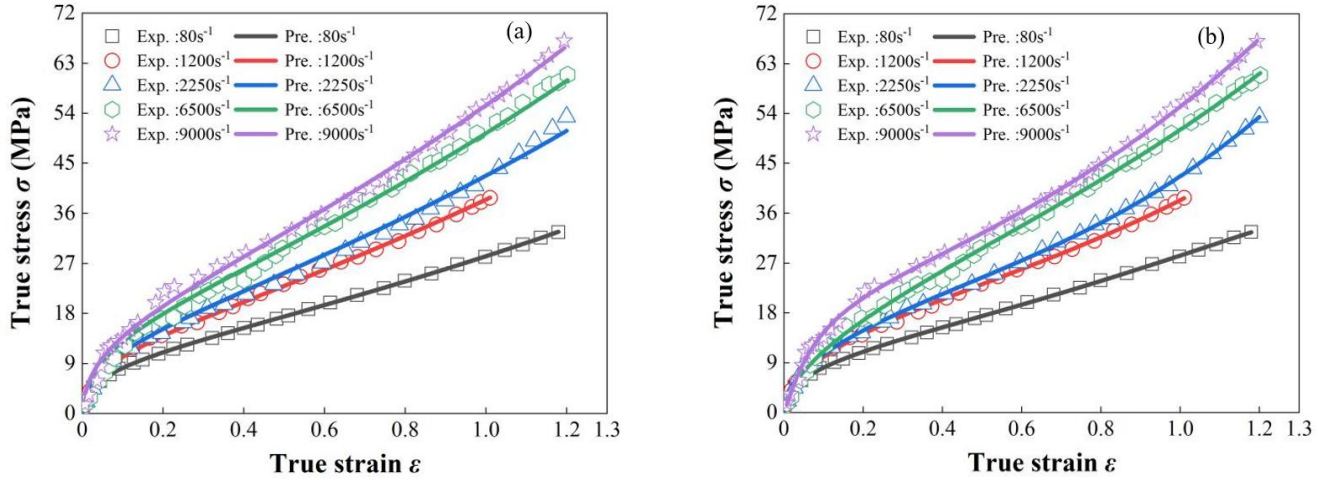

Fig. 13: Omparision between proposed and strain-dependent fractional-order constitutive models at different strain rates. (The experimental data are cited from Sarva *et al*.[20] (a) Strain-dependent fractional-order constitutive models and (b) strain rate-dependent fractional-order models.

and the model introduced in this paper were employed to predict the mechanical response curve of PET. The prediction results are presented in Fig. 13. Specifically, Fig. 13(a) demonstrates the predictive capability of the strain-dependent continuous power-law variable-order constitutive model in simulating the stress-strain curve of PET. Conversely, Fig. 13(b) illustrates the predictions of the strain rate-dependent continuous power-law variable-order constitutive model throughout the entire deformation stage of the material's stress-strain response. Through comparison, it can be clearly observed that the model introduced in this paper outperforms the one presented in Fig. 13(a), particularly during the nonlinear large deformation phase under high-speed impact conditions. Notably, the proposed model accurately aligns with the material's deformation response. Furthermore, across a broad range of high strain rates, the prediction curve generated by the proposed model faithfully recapitulates the material's mechanical response, aligning seamlessly with the experimental stress-strain curve. Additionally, both models adhere to the equivalent conversion criterion outlined in Eq. (7):$m = d\tau = d_{ref}\tau_{ref}$, where d_{ref} is selected within a defined boundary range and is set at 80s^{-1}.

Table 5 provides a clear comparison of the RMSE values between the two constitutive models, further confirming the superiority of the proposed strain-rate-dependent continuous power-law variable-order constitutive model in describing the mechanical response of PET materials. The results show that the *RMSE* values of the proposed model are consistently below 0.2%, whereas those of the comparison model are approximately twice as high, highlighting the significant advantage of the proposed model in reducing prediction error. Meanwhile, the RMSE values of both models remain below 0.5% across different strain rates, underscoring their high fitting accuracy within the high strain rate range.

Moreover, the proposed model more accurately captures the strain-rate sensitivity of PET materials, revealing a clear relationship between the material's mechanical properties and strain rate. Specifically, the stress-strain response exhibits a power-law growth trend with increasing strain rate, which validates the power-law correlations between material parameters (*e.g.*, elastic modulus, relaxation time) and strain rate as described in Eq. (13). The findings are further supported by Table 6, which shows that the adjusted R_a^2 of the proposed model consistently exceeds that of the comparison model under different high strain rate conditions. However, the difference in fitting accuracy between the two models is minimal, approximately on the order of 10^{-4}. Notably, at a strain rate of 6500 s^{-1} , the difference reaches its smallest value of 4.3×10^{-4}. This result indicates that while both models exhibit high fitting accuracy at high strain rates, the predictions of the proposed model align more closely with the experimental true values. Furthermore, its prediction error for polymers remains consistent with that under low strain rate conditions, generally below 0.05%. In summary, by monitoring changes in strain rate, the proposed model can accurately capture the overall mechanical response parameters of the material. This capability enables the proposed model to excel in real-time identification and prediction of the nonlinear large deformation characteristics of PET and elastomer polymers, providing a reliable tool for further research.

4.3 Demonstration of the application of the proposed model in prediction within a wide strain rate range

The preceding chapters have delved into the predictive capabilities of the proposed model in capturing the temporal evolution of material mechanical responses across both low and high strain rate conditions. On this basis, this section broadens the scope of strain rate investigation, aiming to comprehensively verify the applicability of the model to strain rate-sensitive materials across a broad range of strain rates, while also delving deeper into the accuracy of its predictions pertaining to the nonlinear large deformation mechanical evolution characteristics influenced by strain rates. Prior chapters primarily focused on the compression and impact

Table 5: The RMSE values of experimental data predicted by two constitutive models under high strain rate.

Models	RMSE at different strain rates				
	80s^{-1}	1200s^{-1}	2250s^{-1}	6500s^{-1}	9000s^{-1}
$\alpha = k\varepsilon^b + Z$	0.00025	0.00123	0.00111	0.00167	0.00253
$\alpha = k_0\varepsilon^b + k_1\dot{\varepsilon}^u + Z_0$	0.00012	0.00063	0.00067	0.00124	0.00092

Table 6: R_a^2 values of two constitutive models under high strain rate.

Models	R_a^2 at different strain rates ($0\leq R_a^2\leq1$)				
	80s^{-1}	1200s^{-1}	2250s^{-1}	6500s^{-1}	9000s^{-1}
$\alpha = k\varepsilon^b + Z$	0.99975	0.99877	0.99889	0.99833	0.99847
$\alpha = k_0\varepsilon^b + k_1\dot{\varepsilon}^u + Z_0$	0.99986	0.99937	0.99933	0.99876	0.99908

compression test data of PET outlined in literature.[13] Conversely, this section introduces tensile test data encompassing variable strain rates, offering a detailed examination of the transition of PET from rubbery behavior at a low strain rate of $0.15s^{-1}$ to leathery characteristics at a high strain rate of $573s^{-1}$. As shown in Fig. 14, the stress exhibits an exponential relationship with strain. Initially, within a narrow strain range, the material undergoes both strain softening and strain hardening stages, where the growth of stress response lags behind the corresponding changes in strain, exhibiting a gradual upward trend. However, as high strain and large deformation phenomena emerge, the stress begins to demonstrate characteristics of nonlinear rapid growth. Furthermore, as the strain rate increases, the mechanical response of the stress-strain relationship is progressively enhanced, with the stress-strain curve at a high strain rate of $573s^{-1}$ significantly exceeding that at a low strain rate of $0.15s^{-1}$. Notably, all stress-strain curves exhibit a continuous power-law trend, indicating that the constitutive properties of the material, including the stress-strain relationship, vary with changes in strain rate.

By comparing the prediction curve of the strain-dependent continuous power-law variable-order constitutive model depicted in Fig. 14(a) with the stress-strain prediction curve of the proposed model under a wide range of strain rates shown in Fig. 14(b), it can be found that the prediction curve of the proposed model aligns perfectly with the experimental data. Furthermore, the predictive ability of the proposed model significantly surpasses that of the comparative model, particularly during the stages of small and medium strain deformation. The comparative model fails to accurately predict the stress response of the material, whereas the proposed model effectively tracks the stress-strain response in real-time. Combining with the *RMSE* values presented in Table 7, it is apparent that the RMSE of the proposed model is lower than that of the comparative model. The average difference in RMSE between the two models across five strain rates stands at a mere 0.0068%, indicating minimal error. However, the proposed model holds greater practical physical significance as it characterizes the evolution of mechanical constitutive parameters of rubber polymers with varying strain rates. This validates the applicability of the proposed strain rate-dependent continuous power-law variable-order constitutive model across a broad range of strain rates, enabling accurate prediction and description of the stress-strain mechanical response of elastomer polymers.

Table 7: RMSE of tensile test data fitted by two constitutive models.

Models	RMSE at different strain rates				
	$0.15s^{-1}$	$14s^{-1}$	$327s^{-1}$	$408s^{-1}$	$573s^{-1}$
$\alpha = k\varepsilon^b + Z$	0.00044	0.00163	0.00047	0.00061	0.00078
$\alpha = k_0\varepsilon^b + k_1\dot{\varepsilon}^u + Z_0$	0.00038	0.00155	0.00041	0.00055	0.0007

Table 8: R_a^2 of tensile test data fitted by two constitutive models.

Models	R_a^2 at different strain rates				
	$0.15s^{-1}$	$14s^{-1}$	$327s^{-1}$	$408s^{-1}$	$573s^{-1}$
$\alpha = k\varepsilon^b + Z$	0.99956	0.99837	0.99953	0.99939	0.99922
$\alpha = k_0\varepsilon^b + k_1\dot{\varepsilon}^u + Z_0$	0.99958	0.99845	0.99956	0.99942	0.9993

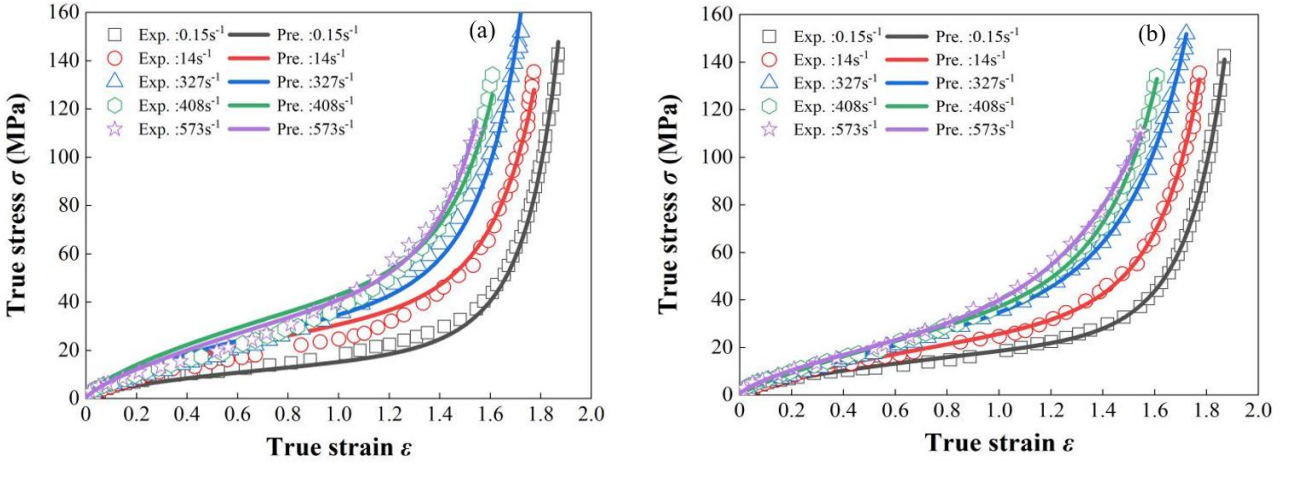

Fig. 14: Comparison of tensile test data under wide strain rate between the proposed model and strain dependent constitutive model (a) Strain-dependent fractional-order constitutive models and (b) strain rate-dependent fractional-order models (the experimental data are quoted from Ref. [13]).

Table 8 further validates the applicability of the propose model across a wide range of strain rates. The R_a^2 values of the proposed model are consistently slightly higher than those of the comparison model across all strain rates, indicating its superior adaptability to experimental data within a broad strain rate range. Notably, as the strain rate increases, the proposed model more accurately captures the mechanical response of the material, with prediction errors consistently below 0.05%. This demonstrates that the introduction of the strain rate function parameters $k_1 \dot{\varepsilon}^u$ and Z_0 enhances the model's flexibility and accuracy in fitting complex datasets.

Overall, while both models exhibit high fitting accuracy, the proposed model demonstrates superior applicability and predictive capability across a wide range of strain rates. The incorporation of strain rate-dependent parameters ensures more stable fitting precision under varying strain rates. This is particularly evident at high strain rates, where the proposed model's predictions align more closely with experimental results. Therefore, the proposed model is better suited for comprehensively describing the strain rate-dependent mechanical behavior of PET materials and elastomer polymers.

5. Conclusion

In this paper, a novel strain rate-dependent fractional-order constitutive model, suitable for a broad range of strain rates, is introduced. Firstly, the nonlinear behavior of elastomer polymers is meticulously analyzed using quasi-static compression, tension, and dynamic compression test data. The influence and relative weights of the constitutive model's constituent parameters on the material's stress-strain mechanical response are thoroughly discussed. Subsequently, strain rate-dependent function models for each parameter are established, with a particular focus on the strain rate-dependent power-law model for the fractional order, which exhibits the greatest influence. Furthermore, a fully strain rate-dependent variable fractional-order constitutive model is developed. The validity and applicability of the proposed model across various strain rate ranges are then evaluated using compression and tension test data from both single rubber materials and rubber polymers in diverse conditions. These results are contrasted with existing strain-related variable fractional-order constitutive models, demonstrating the predictive accuracy and physical relevance of the proposed model. The main conclusions of this paper are as follows:

(1) A new continuous power-law variable fractional-order model has been developed to predict the strain rate-dependent mechanical properties of materials. This model demonstrates superior accuracy and precision in characterizing the nonlinear stress-strain relationship of specific elastomer polymers compared to traditional models. It also effectively addresses the strain rate sensitivity of elastomer polymers, reducing parameter uncertainty and error. The model comprehensively captures the mechanical evolution of materials, particularly during nonlinear large deformation behavior, highlighting its distinct advantages and wide application potential.

(2) Taking into account the influence of strain rate on elastic modulus and relaxation time, a continuous power-law fractional-order constitutive model with comprehensive strain rate correlation is proposed. By comparing the static and dynamic compression test data of the material across low and high strain rates, it is found that the global stress-strain response of the material exhibits a correlation with strain rate, and the constitutive properties, including elastic modulus and relaxation time, vary accordingly. Furthermore, a comparative analysis reveals that the proposed model outperforms the traditional one in terms of prediction accuracy, better aligning with the constitutive characteristics and physical significance of rubber polymers across varying strain rates. Specifically, at a low strain rate of $0.005s^{-1}$, the RMSE value of the comparison model is 4.77 times higher than that of the proposed model, while at high strain rates of $9000s^{-1}$, it is twice as high. Notably, both constitutive models demonstrate low RMSE values (less than 0.5%) across different strain rates.

(3) Across a broad range of strain rates, the proposed model exhibits not only remarkable prediction accuracy but also consistently low prediction errors, all falling below 0.05%. This precision significantly surpasses that of strain-dependent variable fractional order constitutive models. Furthermore, the model demonstrates extensive applicability, as evidenced by its accurate portrayal of the mechanical characteristics of various elastomer polymers in predicting the mechanical response curves of rubber, polyurea, and PET materials, maintaining a prediction accuracy of over 99.5% consistently.

Acknowledgments

The work described in this paper was supported by Natural Science Foundation of China project (Grant No.52302475) , Shanxi Provincial Basic Research Program Joint Funding Project (TZLH20230818002).

Conflict of Interest

There is no conflict of interest.

Supporting Information

Not applicable.

Nomenclatures

RMSE	Root Mean Squared Error
PET	Polyethylene terephthalate
FKM	fluororubber
SR	silicon rubber
E	defined in Eq. (1), [MPa]
t	defined in Eq. (1), [s]
$\dot{\varepsilon}$	defined in Eq. (4), [s^{-1}]
k	defined in Eq. (6)
b	defined in Eq. (6)
Z	defined in Eq. (6)
v	defined in Eq. (9)
d	defined in Eq. (9), [s^{-1}]

d_{ref}	defined in Eq. (9), [s^{-1}]
R_a^2	Fit correlation coefficient R^2
PE	polyurea elastomer

Greek symbols

τ	defined in Eq. (1), [s]
σ	stress, [MPa]
ε	strain
α	defined in Eq. (1)
Γ	defined in Eq. (2)
λ	defined in Eq. (9)

References

[1] P. Gao, T. Yu, Y. Zhang, J. Wang, J. Zhai, Vibration analysis and control technologies of hydraulic pipeline system in aircraft: a review, *Chinese Journal of Aeronautics*, 2021, **34**, 83-114, doi: 10.1016/j.cja.2020.07.007.

[2] H. Teimouri, R. T. Faal, A. S. Milani, Impact response of fractionally damped rectangular plates made of viscoelastic composite materials, *Applied Mathematical Modelling*, 2025, **137**, 115678, doi: 10.1016/j.apm.2024.115678.

[3] J. Marais, G. Venter, Numerical modelling of the temperature distribution in the cross-section of an earthmover tyre, *Applied Mathematical Modelling*, 2018, **57**, 360-375, doi: 10.1016/j.apm.2018.01.018.

[4] Z. Zhao, W. Meng, B. Yan, T. Yang, H. Ren, Y. Yuan, Optimization design of vibration reduction structure of driving sprocket based on niche adaptive genetic algorithm, *International Journal of Acoustics and Vibration*, 2022, **27**, 162, doi: 10.20855/ijav.2022.27.21851.

[5] L. Benea, L. Mardare, N. Simionescu, Anticorrosion performances of modified polymeric coatings on E32 naval steel in sea water, *Progress in Organic Coatings*, 2018, **123**, 120-127, doi: 10.1016/j.porgcoat.2018.06.020.

[6] A. Stoddart, Polymers: phosphorus analogues of rubber, *Nature Reviews Materials*, 2017, **2**, 17055, doi: 10.1038/natrevmats.2017.55.

[7] S. Ge, S. Samanta, B. Li, G. P. Carden, P. F. Cao, A. P. Sokolov, Unravelling the mechanism of viscoelasticity in polymers with phase-separated dynamic bonds, *ACS Nano*, 2022, **16**, 4746-4755, doi: 10.1021/acsnano.2c00046.

[8] S. Reese, A micromechanically motivated material model for the thermo-viscoelastic material behaviour of rubber-like polymers, *International Journal of Plasticity*, 2003, **19**, 909-940, doi: 10.1016/S0749-6419(02)00086-4.

[9] A. Wang, F. Vargas-Lara, J. M. Younker, K. A. Iyer, K. R. Shull, S. Keten, Quantifying chemical composition and cross-link effects on EPDM elastomer viscoelasticity with molecular dynamics, *Macromolecules*, 2021, **54**, 6780-6789, doi: 10.1021/acs.macromol.1c00162.

[10] J. T. Fan, J. Weerheijm, L. J. Sluys, Compressive response of a glass–polymer system at various strain rates, *Mechanics of Materials*, 2016, **95**, 49-59, doi: 10.1016/j.mechmat.2015.12.005.

[11] I. C. Tsimouri, F. Schwarz, T. Bernhard, A. A. Gusev, A comparison between predictions of the miller-macosko theory, estimates from molecular dynamics simulations, and long-standing experimental data of the shear modulus of end-linked polymer networks, *Macromolecules*, 2024, **57**, 4273-4284, doi: 10.1021/acs.macromol.3c02544.

[12] H. Cho, J. Lee, J. Moon, E. Pöselt, P. J. I. Veld, G. C. Rutledge, M. C. Boyce, Large strain micromechanics of thermoplastic elastomers with random microstructures, *Journal of the Mechanics and Physics of Solids*, 2024, **187**, 105615, doi: 10.1016/j.jmps.2024.105615.

[13] J. Yi, M. C. Boyce, G. F. Lee, E. Balizer, Large deformation rate-dependent stress-strain behavior of polyurea and polyurethanes, *Polymer*, 2006, **47**, 319-329, doi: 10.1016/j.polymer.2005.10.107.

[14] A. F. M. S. Amin, A. Lion, S. Sekita, Y. Okui, Nonlinear dependence of viscosity in modeling the rate-dependent response of natural and high damping rubbers in compression and shear: Experimental identification and numerical verification, *International Journal of Plasticity*, 2006, **22**, 1610-1657, doi: 10.1016/j.ijplas.2005.09.005.

[15] Y. Pan, Z. Zhong, A viscoelastic constitutive modeling of rubber-like materials with the Payne effect, *Applied Mathematical Modelling*, 2017, **50**, 621-632, doi: 10.1016/j.apm.2017.06.018.

[16] J. A. López-Campos, A. Segade, J. R. Fern ndez, E. Casarejos, J. A. Vil n, Behavior characterization of visco-hyperelastic models for rubber-like materials using genetic algorithms, *Applied Mathematical Modelling*, 2019, **66**, 241-255, doi: 10.1016/j.apm.2018.08.031.

[17] P. Zhang, A. C. To, Transversely isotropic hyperelastic-viscoplastic model for glassy polymers with application to additive manufactured photopolymers, *International Journal of Plasticity*, 2016, **80**, 56-74, doi: 10.1016/j.ijplas.2015.12.012.

[18] E. P. Motta, J. M. L. Reis, H. S. da Costa Mattos, Modelling the cyclic elasto-viscoplastic behaviour of polymers, *Polymer Testing*, 2019, **78**, 105991, doi: 10.1016/j.polymertesting.2019.105991.

[19] M. C. Boyce, S. Socrate, P. G. Llana, Constitutive model for the finite deformation stress–strain behavior of poly(ethylene terephthalate) above the glass transition, *Polymer*, 2000, **41**, 2183-2201, doi: 10.1016/S0032-3861(99)00406-1.

[20] S. S. Sarva, S. Deschanel, M. C. Boyce, W. Chen, Stress-strain behavior of a polyurea and a polyurethane from low to high strain rates, *Polymer*, 2007, **48**, 2208-2213, doi: 10.1016/j.polymer.2007.02.058.

[21] Y. Miao, H. Zhang, H. He, Q. Deng, Mechanical behaviors and equivalent configuration of a polyurea under wide strain rate range, *Composite Structures*, 2019, **222**, 110923, doi: 10.1016/j.compstruct.2019.110923.

[22] J. Richeton, S. Ahzi, K. S. Vecchio, F. C. Jiang, A. Makradi, Modeling and validation of the large deformation inelastic response of amorphous polymers over a wide range of temperatures and strain rates, *International Journal of Solids and Structures*, 2007, **44**, 7938-7954, doi: 10.1016/j.ijsolstr.2007.05.018.

[23] C. A. Bernard, O. Lame, T. Deplancke, J. Y. Cavaillé, K.

Ogawa, From rheological to original three-dimensional mechanical modelling of semi-crystalline polymers: Application to a wide strain rate range and large deformation of ultra-high molecular weight polyethylene, *Mechanics of Materials*, 2020, **151**, 103640, doi: 10.1016/j.mechmat.2020.103640.
[24] Z. Qi, N. Hu, G. Li, D. Zeng, X. Su, Constitutive modeling for the elastic-viscoplastic behavior of high density polyethylene under cyclic loading, *International Journal of Plasticity*, 2019, **113**, 125-144, doi: 10.1016/j.ijplas.2018.09.010.
[25] L. E. S. Ramirez, C. F. M. Coimbra, A variable order constitutive relation for viscoelasticity, *Annalen der Physik*, 2007, **519**, 543-552, doi: 10.1002/andp.200751907-803.
[26] R. Meng, D. Yin, C. S. Drapaca, A variable order fractional constitutive model of the viscoelastic behavior of polymers, *International Journal of Non-Linear Mechanics*, 2019, **113**, 171-177, doi: 10.1016/j.ijnonlinmec.2019.04.002.
[27] H. Khajehsaeid, J. Arghavani, R. Naghdabadi, S. Sohrabpour, A visco-hyperelastic constitutive model for rubber-like materials: a rate-dependent relaxation time scheme, *International Journal of Engineering Science*, 2014, **79**, 44-58, doi: 10.1016/j.ijengsci.2014.03.001.
[28] P. Yu, X. Yao, S. Tan, Q. Han, A macro-damaged viscoelastoplastic model for thermomechanical and rate-dependent behavior of glassy polymers, *Macromolecular Materials and Engineering*, 2016, **301**, 469-485, doi: 10.1002/mame.201500322.
[29] X. Wang, W. Peng, Y. Hu, M. Yang, D. Han, C. Ma, Y. Lin, H. Wang, R. Zhang, Z. Zhang, G. Shao, High-pressure synthesis of fully dense polymer-derived SiCN ceramics: Structural evolution and mechanical properties, *Journal of the European Ceramic Society*, 2024, **44**, 116760, doi: 10.1016/j.jeurceramsoc.2024.116760.
[30] K. B. Bhagavathula, C. S. Meredith, S. Ouellet, D. L. Romanyk, J. D. Hogan, Density, strain rate and strain effects on mechanical property evolution in polymeric foams, *International Journal of Impact Engineering*, 2022, **161**, 104100, doi: 10.1016/j.ijimpeng.2021.104100.
[31] T. Su, H. Zhou, J. Zhao, Z. Liu, D. Dias, A fractional derivative-based numerical approach to rate-dependent stress-strain relationship for viscoelastic materials, *Acta Mechanica*, 2021, **232**, 2347-2359, doi: 10.1007/s00707-021-02946-1.
[32] W. Cai, P. Wang, Rate-dependent fractional constitutive model for nonlinear behaviors of rubber polymers, *European Journal of Mechanics - A/Solids*, 2024, **103**, 105186, doi: 10.1016/j.euromechsol.2023.105186.
[33] R. M. Christensen, Chapter I, Viscoelastic stress strain constitutive relations, Theory of Viscoelasticity, California, 1982, 20-33, ISBN: 9780121742522.
[34] C. M. Roland, J. N. Twigg, Y. Vu, P. H. Mott, High strain rate mechanical behavior of polyurea, *Polymer*, 2007, **48**, 574-578, doi: 10.1016/j.polymer.2006.11.051.
[35] Z. Yousaf, M. Smith, P. Potluri, W. Parnell, Compression properties of polymeric syntactic foam composites under cyclic loading, *Composites Part B: Engineering*, 2020, **186**, 107764, doi: 10.1016/j.compositesb.2020.107764.